Molecular Pharmacology Fast Forward. Published on June 10, 2009 as doi:10.1124/mol.109.056663
This article has not been copyedited and formatted. The final version may differ from this version.

Title:

Selective Activation of the SK1 Subtype of Human Small Conductance Ca^{2+}-Activated K^+ Channels by GW542573X is Dependent on Serine 293 in the S5 Segment

Authors:

Charlotte Hougaard, Marianne L. Jensen, Tim J. Dale, David D. Miller, David J. Davies, Birgitte L. Eriksen, Dorte Strøbæk, Derek J. Trezise, Palle Christophersen

Addresses:

NeuroSearch A/S, Pederstrupvej 93, DK 2750 Ballerup, Denmark. **(**C.H., M.L.J., B.L.E., D.S., P.C.)

GlaxoSmithKline, Medicines Research Centre, Gunnels Wood Road, Stevenage, Hertfordshire SG1 2NY, United Kingdom. (T.J.D., D.J.T., D.D.M., D.J.D.).

Molecular Pharmacology Fast Forward. Published on June 10, 2009 as DOI: 10.1124/mol.109.056663
This article has not been copyedited and formatted. The final version may differ from this version.

Running title: Selective activation of SK1 channels by GW542573X

Corresponding author:

Palle Christophersen

NeuroSearch A/S, Pederstrupvej 93, DK 2750 Ballerup, Denmark

Tel: +45 44 60 82 22

Fax: +45 44 60 80 80

E-mail: pc@neurosearch.dk

Text pages:	**23**
Number of tables:	**0**
Number of figures:	**8**
Number of references:	**28**
Words in Abstract:	**275**
Words in Introduction:	**643**
Words in Discussion:	**1286**

Abbreviations: BK channel, big conductance Ca^{2+}-activated K^+ channel; BMB, bicuculline methobromide; CaM, calmodulin; CaMBD, calmodulin binding domain; CHO cells, Chinese hamster ovary cells; CK2, casein kinase 2; CNS, central nervous system; CyPPA, cyclohexyl-[2-(3,5-dimethyl-pyrazol-1-yl)-6-methyl-pyrimidin-4-yl]-amine; DCEBIO, 5,6-Dichloro-1-ethyl-1,3-dihydro-benzoimidazol-2-one; DCM, dichloromethane; DMSO, dimethylsulfoxide; 1-EBIO, 1-ethyl-2-benzimidazolinone; FRET, fluorescence resonance energy transfer; GW542573X, 4-(2-Methoxy-phenylcarbamoyloxymethyl)-piperidine-1-carboxylic acid *tert*-butyl ester; HEK293 cells, human embryonic kidney cells; IK channel, intermediate conductance Ca^{2+}-activated K^+ channel; MOA, mode of action; NS309, 6,7-dichloro-1*H*-indole-2,3-dione 3-oxime; NS8593, (*R*)-*N*-(benzimidazol-2-yl)-1,2,3,4-tetrahydro-1-naphtylamine; PBS, phosphate buffered saline; PP2A, phospatase 2A; S, transmembrane segment; SKA-31, naphtha[1,2-*d*]thiazol-2-ylamine; SK channel, small conductance Ca^{2+}-activated K^+ channel; VIPR, voltage ion prope reader; CC2-DMPE, CC-2-dimyristoyl phosphatidylethanolamine; $DiSBAC_2(3)$, bis-(1,3-diethylthiobarbituric acid) trimethine oxonol.

Molecular Pharmacology Fast Forward. Published on June 10, 2009 as DOI: 10.1124/mol.109.056663
This article has not been copyedited and formatted. The final version may differ from this version.

ABSTRACT

A new small molecule, 4-(2-methoxy-phenylcarbamoyloxymethyl)-piperidine-1-carboxylic acid *tert*-butyl ester (GW542573X), is presented as an activator of small conductance Ca^{2+}-activated K^+ (SK, $K_{Ca}2$) channels and distinguished from previously published positive modulators of SK channels, such as 1-EBIO and CyPPA, in several aspects. GW542573X is the first SK1-selective compound described: An EC_{50} value of 8.2 ± 0.8 µM (n = 6, $[Ca^{2+}]_i$ = 200 nM) was obtained from inside-out patches excised from hSK1-expressing HEK293 cells. Whole-cell experiments showed that hSK2 and hSK3 channels were more than 10 times, and hIK channels even more than 100 times, less sensitive to GW542573X. The Ca^{2+} response curve of hSK1 was left-shifted from an $EC_{50}(Ca^{2+})$ value of 410 ± 20 nM (n = 9) to 240 ± 10 nM (n = 5) in the presence of 10 µM GW542573X. In addition to this positive modulation, GW542573X activated SK1 in the absence of Ca^{2+} and furthermore induced a 15% increase in the maximal current at saturating Ca^{2+}. Thus, GW542573X also acts as a genuine opener of the hSK1 channels, a mechanism of action (MOA) not previously obtained with SK channels. The differential potency on hSK1 and hSK3 enabled a chimera approach to elucidate site(s) important for this new MOA and selectivity property. A single amino acid (S293) located in S5 of hSK1 was essential and substituting the corresponding L476 in hSK3 with serine conferred hSK1-like potency (EC_{50} = 9.3 ± 1.4 µM (n = 5)). GW542573X may activate SK channels via interaction with “deep pore” gating structures at the inner pore vestibule or the selectivity filter, in contrast to 1-EBIO and CyPPA that exert positive modulation via the intracellular calmodulin binding domain (CaMBD).

Molecular Pharmacology Fast Forward. Published on June 10, 2009 as DOI: 10.1124/mol.109.056663
This article has not been copyedited and formatted. The final version may differ from this version.

Small conductance Ca^{2+}-activated K^+ channels (SK channels) are voltage-independent channels being gated solely by intracellular Ca^{2+}. Three subtypes of SK channels have been described (SK1-SK3, $K_{Ca}2.1$-$K_{Ca}2.3$; for review see Stocker, 2004), which together with the related Ca^{2+}-activated K^+ channel of intermediate conductance (IK, $K_{Ca}3.1$), acquire their Ca^{2+}-sensitivity from C-terminally attached calmodulin (CaM) (Köhler et al., 1996; Xia et al., 1998; Khanna et al., 1999). All SK subtypes possess nearly identical Ca^{2+}-response curves (EC_{50} ~ 400 nM; n_{Hill} ~ 5). The high Hill value may indicate cooperative binding of Ca^{2+}, since each of the 4 SK α-subunits is associated with CaM capable of binding up to 2 Ca^{2+} (Schumacher et al., 2001). Fast and high-affinity responses to changes in the intracellular Ca^{2+} concentration ($[Ca^{2+}]_i$) are the basis for functional coupling of SK channels to specific localized Ca^{2+} transients in different neurons, and for their participation in neurophysiological processes like spike frequency adaptation, pacemaking, as well as synaptic integration and plasticity (for reviews see Bond et al., 2005; Pedarzani and Stocker, 2008).

Gating of SK channels can be modulated by physiological and pharmacological means. SK2 and SK3 channels are part of multiheteromeric protein complexes consisting of CaM, casein kinase 2 (CK2), phosphatase 2A (PP2A) as well as scaffolding proteins. CK2 and PP2A oppositely regulate the apparent Ca^{2+}-sensitivity by phosphorylating/dephosphorylating CaM at threonine 80 (Bildl et al., 2004; Allen et al., 2007). Recently, this system was shown to respond to the activation of noradrenaline receptors causing phosphorylation of CaM, reduced SK channel Ca^{2+}-sensitivity, and functional uncoupling to Ca^{2+} influx mediated by P/Q Ca^{2+} channels (Maingret et al., 2008). Similar processes may underlie the sigma-1 receptor-mediated inhibition of SK channels that facilitate induction of long term potentiation in the hippocampus (Martina et al., 2007). Small molecules like NS8593 ((*R*)-*N*-

Molecular Pharmacology Fast Forward. Published on June 10, 2009 as DOI: 10.1124/mol.109.056663
This article has not been copyedited and formatted. The final version may differ from this version.

(benzimidazol-2-yl)-1,2,3,4-tetrahydro-1-naphtylamine) (Strøbæk et al., 2006) and its analogues (Sørensen et al., 2008) also possess the ability to inhibit SK channels by shifting the Ca^{2+}-response curve to the right (apparent reduced Ca^{2+}-sensitivity), an inhibitory principle called negative gating modulation. This differs mechanistically from the action of apamin, a selective pore blocker of SK channels. In contrast, 1-EBIO (1-ethyl-2-benzimidazolinone), NS309 (6,7-dichloro-1*H*-indole-2,3-dione 3-oxime) and SKA-31 (naphtha[1,2-*d*]thiazol-2-ylamine) positively modulates IK and SK channels (IK>SK1=SK2=SK3) by shifting their Ca^{2+}-response curves to the left (apparent increased Ca^{2+}-sensitivity), without exerting agonism *per se* (Pedarzani et al., 2001; Hougaard et al., 2007; Sankaranarayanan et al., 2009). Even though clear molecular and mechanistic differences exist, positive gating modulation may qualitatively resemble the physiological effects of PP2A-mediated increased Ca^{2+}-sensitivity described for SK2/SK3 channels. Despite the highly homologous gating mechanisms shared by all SK subtypes, pharmacological modulation can be subtype-selective as illustrated by the compound CyPPA (cyclohexyl-[2-(3,5-dimethyl-pyrazol-1-yl)-6-methyl-pyrimidin-4-yl]-amine), which is active on hSK3 and hSK2 channels, while inactive on hSK1 or hIK (hSK3>hSK2>>hSK1=hIK) (Hougaard et al., 2007). The effects of CyPPA and 1-EBIO have, from their actions on hSK3/hSK1 or SK2/IK chimeras, been shown to depend on the CaMBD in the C-terminal.

Here we describe a new activator of hSK channels, 4-(2-methoxy-phenylcarbamoyloxymethyl)-piperidine-1-carboxylic acid *tert*-butyl ester (GW542573X), which is unique in several respects: First, this compound demonstrates a novel selectivity profile, being selective for hSK1 over hSK2 and hSK3 and virtually inactive on hIK (hSK1>hSK2=hSK3>hIK). Second, it partially activates hSK1 even in the absence of intracellular Ca^{2+}. Third, this compound does

Molecular Pharmacology Fast Forward. Published on June 10, 2009 as DOI: 10.1124/mol.109.056663
This article has not been copyedited and formatted. The final version may differ from this version.

not act via the intracellular CaMBD, but via a transmembrane segment (S5). Fourth, remarkably, loss-of-sensitivity is achievable by substituting the hSK1 serine residue with the equivalent hSK3 leucine residue (S293L), whereas gain-of-sensitivity is achievable by the reverse mutation in hSK3 (L476S). Thus, GW542573X is the first representative of a new chemical and functional class of SK channel activators. The identification of a molecular determinant for SK channel activation positioned close to the inner pore cavity and selectivity filter is discussed in relation to the proposed "deep pore" mechanism for gating of SK channels (Bruening-Wright et al., 2002; Bruening-Wright et al., 2007).

Molecular Pharmacology Fast Forward. Published on June 10, 2009 as DOI: 10.1124/mol.109.056663
This article has not been copyedited and formatted. The final version may differ from this version.

Materials and Methods

Chemistry

GW542573X was prepared at GlaxoSmithKline (Stevenage, UK) by the following procedure. 4-Hydroxymethyl-piperidine-1-carboxylic acid *tert*-butyl ester (1.0 equiv.) in anhydrous dichloromethane (DCM) at 0°C under a nitrogen atmosphere was treated with sodium hydride (1.05 equiv.) and then stirred at 0°C for 1 h. 2-Methoxyphenyl isocyanate (1.0 equiv.) was added and the reaction stirred for 18 h at ambient temperature. The reaction was quenched with saturated aqueous sodium bicarbonate solution, diluted with an equal volume of DCM and washed with saturated aqueous sodium bicarbonate solution. The organic layer was separated, dried over anhydrous $MgSO_4$ and evaporated *in vacuo*. The crude product was purified in small quantities by mass directed HPLC, or in larger quantity by silica chromatography, eluting with cyclohexane:ethyl acetate 9:1. The purified product was obtained as a colourless oil which slowly crystallised to a white solid on standing. MH^+ 365 (100 %), MNH_4^+ 382 (100%), 265 (40%). (Dale, T J, Davies D J, Trezise, D J, WO2004/014425 (2004)).

NS309 (Strøbæk et al., 2004) was synthesized at NeuroSearch A/S (Ballerup, Denmark). GW542573X and NS309 were dissolved in DMSO and diluted to the final concentration in the experimental solution. Apamin (Sigma-Aldrich) was dissolved in the experimental solution and bicuculline methobromide (Biomedicals Inc. (Illkirch, France) in DMSO.

Cell cultures

For the patch clamp experiments HEK293 cell lines stably expressing hSK1, hSK2, hSK3 and hIK channels were used. cDNA encoding hSK1 was constructed as described in (Strøbæk et al., 2000) (UniProtKB/Swiss-Prot Q92952) and was

Molecular Pharmacology Fast Forward. Published on June 10, 2009 as DOI: 10.1124/mol.109.056663
This article has not been copyedited and formatted. The final version may differ from this version.

subcloned into the custom made expression vector pNS1n derived from pcDNA3. Stable hSK1 HEK293 cell lines were isolated using G418 as a selection marker. pcDNA3_hSK2, a kind gift from B. Attali (Desai et al., 2000; UniProtKB/Swiss-Prot Q9H2S1), was used to generate HEK293 cells stably expressing hSK2. hSK3 expressing HEK293 cell lines were based on the plasmid pNS3n_hSK3 previously described in (Strøbæk et al., 2004; UniProtKB/Swiss-Prot Q9UG16). cDNA encoding hIK (Jensen et al., 1998; UniProtKB/Swiss-Prot O15554) was subcloned using EcoRI and XhoI into pNS1n, and stable HEK293 cell lines were selected using G418. Expression of hSK1, hSK2, hSK3 and hIK were verified by patch-clamp measurements. Channel chimeras and point mutated channels (see below) were transiently transfected into HEK293 cells using Lipofectamine (Invitrogen) and standard transfection methods. Electrophysiological measurements were performed 2-3 days after the transfection. Cells were cultured in Dulbecco's Modified Eagle's Medium (DMEM, Sigma-Aldrich, Brøndby, Denmark) supplemented with 10% fetal calf serum (FCS, Gibco, Invitrogen, NY, USA) at 37°C and 5% CO_2. At approximately 75% confluence, the cells were washed once with phosphate buffered saline (PBS), harvested by trypsin/EDTA (Sigma-Aldrich) treatment and transferred to petri dishes containing cover slips (∅ 3.5 mm, purchased from VWR international, Herlev, Denmark).

For the voltage ion probe reader (VIPR) experiments, hSK1-CHO cells were used (see Dale et al., 2002). Stable cell lines were cultured under selection for resistance to 500 μg ml^{-1} geneticin in α-MEM (Gibco BRL) with 10% heat inactivated foetal bovine serum (Gibco BRL) at 37°C and 5% CO_2. 2-4 days prior to the experiment cells were plated in black walled clear bottom sterile 96 well plates (Costar) at a density of 50K cells per well.

Molecular Pharmacology Fast Forward. Published on June 10, 2009 as DOI: 10.1124/mol.109.056663
This article has not been copyedited and formatted. The final version may differ from this version.

Molecular biology

Three unique restriction sites were introduced in conserved regions of hSK1 and hSK3 at the following amino acid positions: SalI at hSK1 L148 and hSK3 L331; HinDIII at hSK1 S190 and hSK3 S373; and AgeI at hSK1 T350 and hSK3 T533. Briefly, hSK1 and hSK3 cDNAs were subcloned into the pcDNA3 derived vectors pNS3n and pNS3h, respectively, using EcoRI and BamHI. All restriction enzymes were purchased from New England Biolabs (USA). These plasmids were uracilated via E.coli RZ1032 (Stratagene, La Jolla, CA, USA) and used as templates in mutagenesis reactions. Six oligonucleotides (MWG Biotec, Germany) were used to introduce the unique restriction sites:

(1) hSK1SalI: ATGCCTCATCAGCCTgTCgACGGCCATCCTGCTGGG

(2) hSK1HinDIII: GCGCGTGTTCCTCATaagctTAGAGCTGGCAGTGTGC

(3) hSK1AgeI: GTGTGTGCCTGCTCACcGGtATCATGGGAGCTGGC

(4) hSK3SalI: CCTTATCAGTCTGTCgACCATCATCCTTTTG

(5) hSK3HinDIII: GAGCGCATCCTGTACATaAGCtTGGAGATGCTGGTG

(6) hSK3AgeI: GTGTCTGTCTCCTCACcGGtATCATGGGTGCAGGC

The mutagenesis reactions were performed using T7 DNA polymerase and T4 DNA ligase (New England Biolabs, USA). E.coli XL1-Blue (Stratagene) was transformed with an aliquot of the reaction mixture and the resulting plasmid DNA was purified using standard methods. Chimera 1 and 2 were assembled using the AgeI site and Chimera 3 was generated by first introducing the hSK3 part between SalI and HinDIII into Chimera 2 and then to introduce the N-terminal tail of hSK3 with overlapping PCR

Molecular Pharmacology Fast Forward. Published on June 10, 2009 as DOI: 10.1124/mol.109.056663
This article has not been copyedited and formatted. The final version may differ from this version.

(Expand High Fidelity PCR System, Roche, Germany) using the following oligonucleotides: hsk3-hSK1s agtgactatgctCTCATTTTCGGCATGTTT and hsk1-hSK3as gccgaaaatgagAGCATAGTCACTCAGTCG introducing the overlapping PCR-product using an upstream polylinker restriction site and SalI. Chimera 4 was generated by joining N-terminal hSK3 and Chimera 2 in the HinDIII-site. Chimeras 5 to 9 were made by performing mutagenesis on Chimera 3 using the following oligonucleotides:

Chimera 5:

CATAAGCTTAGAGCTactAGTGTGCGCCATTCACCCGaTcCCCGGCgAgTACCG CTTCACGTGG;

Chimera 6:

GCGCGGCTGGCCTTCtCaTAtGCGCCCTCGGTGGCCGAGGCCGACGTGGAtaTc aTaCTGTCCATCCCCATG;

Chimera 7:

CCTGCGCCTCTACCTGaTcGcCCGGGTGATGCTACTG;

Chimera 8:

GGTGATGCTACTGCAttcgAAAcTCTTCACGGACGCCTC and

GGCCCTCAACAAGATtAatTTCAACACGCGCTTC

Chimera 9:

GTGCTGCTGGTCTTCtcgATaTCCctCTGGATCATCGCAGC.

Chimera 10 was generated by mutagenesis on hSK3 using the following oligonucleotide:

CTGTGCTGCTCGTGTTCtcgATaTCTtcGTGGATCATTGCTGCCTG.

All constructs were verified by sequencing (MWG Biotech, Germany).

Molecular Pharmacology Fast Forward. Published on June 10, 2009 as DOI: 10.1124/mol.109.056663
This article has not been copyedited and formatted. The final version may differ from this version.

Membrane potential assays

The membrane potential of hSK1-CHO cells was monitored using fluorescence resonance energy transfer (FRET) between a phospholipid anchored coumarin donor CC-2-dimyristoyl phosphatidylethanolamine (CC2-DMPE) and oxonol acceptor bis-(1,3-diethylthiobarbituric acid) trimethine oxonol ($DisBAC_2(3)$) on a voltage ion probe reader (VIPR, Aurora Biosciences; González et al., 1999). Experiments were performed at room temperature by first washing the cells with an external buffer containing (in mM) 145 NaCl, 5 KCl, 2 $CaCl_2$, 1 $MgCl_2$, 20 HEPES, 10 glucose, pH 7.4 and then incubating with CC2-DMPE (8 μM diluted in external buffer) for 30 min. Cells were then washed to remove unbound coumarin prior to addition of DisBAC2(3) (8 μM in external buffer for 45 min) and ESS Cy4 (350 μM) a background signal fluorescence quenching reagent. The coumarin fluorophore was excited at 405 nM using a Xenon lamp and dual emission measured each second at 460 nm (coumarin) and 580 nm (oxonol). The signal ratio at the two wavelengths was calculated as a measure of the FRET between the two fluorophores. After 5 consecutive baseline readings GW542573X (100 nM-100 μM) was added online and fluorescence was monitored for up to a further 5 min. To determine final Rf/Ri ratios fluorescence values from cell free wells of the microtitre plate were first subtracted.

Electrophysiology

Membrane currents were recorded under voltage-clamped conditions using the whole-cell or the inside-out configuration of the patch-clamp technique. Cells seeded on cover slips were transferred to a 15 μl recording chamber continuously perfused at 1 ml min^{-1} at room temperature. The chamber was grounded by an integrated Ag/AgCl

Molecular Pharmacology Fast Forward. Published on June 10, 2009 as DOI: 10.1124/mol.109.056663
This article has not been copyedited and formatted. The final version may differ from this version.

pellet. Patch pipettes (approx. 2 MΩ) were pulled from borosilicate tubes with an outside diameter of 1.32 mm (Vitrex Medical, Herlev, Denmark) using a horizontal electrode puller (Zeitz Instruments, Augsburg, Germany). An electronically controlled micromanipulator (Eppendorf, Radiometer, Denmark) was used for the positioning of pipettes. Experiments were controlled by an EPC-9 amplifier (HEKA, Lambrecht, Germany) connected to a Macintosh computer by an ITC-16 interface. Data were filtered at 3 kHz. Currents were elicited by applying a 200 ms linear voltage ramp from -80 to +80 mV every 5 s from a holding potential of 0 mV. In whole-cell experiments, the cell capacitance and series resistance (R_s below 8 MΩ, 80% compensation) were updated before each voltage ramp.

In all experiments a high K^+ solution was applied to the extracellular side of the membrane (in mM): 154 KCl, 2 $CaCl_2$, 1 $MgCl_2$ and 10 HEPES, pH adjusted to 7.4 with KOH. The intracellular solutions contained (in mM): 154 KCl, 10 HEPES, 10 EGTA, or a combination of EGTA and NTA (10 mM in total). Concentrations of $MgCl_2$ and $CaCl_2$ required to obtain the desired free concentrations (Mg^{2+} always 1 mM, Ca^{2+} 0.01 – 10 µM) were calculated (EqCal, Cambridge, UK) and added. In the nominal Ca^{2+}-free intracellular solution, no Ca^{2+} was added. Intracellular solutions were adjusted to pH 7.2 with concentrated HCl or KOH.

Calculations and statistics

EC_{50} and n_{Hill} values for compounds and Ca^{2+} were estimated from equilibrium concentration-response relationships by fitting to the Hill equation:

$$B(C) = \frac{[B(\text{inf}) - B(0)] * C^n}{EC_{50}^n + C^n} + B(0) \qquad \text{(Eq. 1)}$$

Molecular Pharmacology Fast Forward. Published on June 10, 2009 as DOI: 10.1124/mol.109.056663
This article has not been copyedited and formatted. The final version may differ from this version.

Where B(C) is the response (current or Rf/Ri) at the concentration C; B(inf), the response fitted at saturating concentrations; B(0), the response at zero concentration; and n, the Hill coefficient.

All results are given as the mean ± standard error of the mean (S.E.M.). Tests for significant difference were performed by one-way analysis of variance (ANOVA, and Bonferroni *post hoc* comparison) or Student's *t*-test, as appropriate.

Molecular Pharmacology Fast Forward. Published on June 10, 2009 as DOI: 10.1124/mol.109.056663
This article has not been copyedited and formatted. The final version may differ from this version.

Results

Fig. 1A shows the chemical structure of the novel compound GW542573X (4-(2-Methoxy-phenylcarbamoyloxymethyl)-piperidine-1-carboxylic acid *tert*-butyl ester) that is chemically unrelated to published SK channel modulators.

The activating effects of GW542573X on hSK1 channels were first identified in a VIPR membrane potential screen. As seen in Fig. 1B&C, GW542573X evoked concentration-dependent membrane hyperpolarisations with a mean EC_{50} value of 4.0 ± 0.8 µM (range 1.6 - 12.5 µM) and a Hill coefficient of 2.1 ± 0.3 (range 0.64 to 4.3, n = 23). These effects were observed with three independent synthetic batches of compound. No responses were observed in untransfected CHO cells. To confirm that the hyperpolarising effects of GW542573X observed in the VIPR experiments truly represent activation of SK channels, patch clamp experiments were performed. Fig. 1D shows a study with a multi-channel inside-out patch pulled from an hSK1 expressing HEK293 cell. Current-voltage (IV) relationships were measured at symmetrical $[K^+]$ and with the $[Ca^{2+}]_i$ buffered at 0.2 µM or 10 µM (solid lines) yielding 5 or 100 % activation, respectively. Applying GW542573X (0.1 to 50 µM, dotted lines) to the inside of the patch at a $[Ca^{2+}]_i$ of 0.2 µM, resulted in a concentration-dependent increase in hSK1 current. The characteristic inward rectification of the SK1 current was maintained when the channels were activated by a combination of low Ca^{2+} and GW542573X. Fig. 1E shows the GW542573X concentration-response relationship for hSK1 based on experiments similar to that shown in Fig. 1D. Data were read at -75 mV after attaining a stable current level at each concentration, and analyzed by normalization to the maximal obtainable current measured at 10 µM Ca^{2+}. Fitting data to the Hill equation yielded an EC_{50} value of 8.2 ± 0.8 µM (n = 6) a Hill coefficient of 1.4 ± 0.1, and an efficacy of 76 ± 5% relative to

Molecular Pharmacology Fast Forward. Published on June 10, 2009 as DOI: 10.1124/mol.109.056663
This article has not been copyedited and formatted. The final version may differ from this version.

the current level at infinite $[Ca^{2+}]_i$. For comparison, the SK channel enhancers NS309, DC-EBIO and 1-EBIO activated hSK1 with EC_{50} values of 0.6 ± 0.06 µM (n = 4), 25 ± 2 µM (n = 4) and 650 ± 158 µM (n = 4), respectively (data not shown). The efficacies with respect to saturating Ca^{2+} of these compounds were close to 100%.

In order to investigate the selectivity profile of GW542573X, whole-cell patch clamp experiments were performed using HEK293 cells stably expressing hSK1, hSK2, hSK3 or hIK channels. The whole-cell configuration was chosen since, in our hands, the hIK current exhibited substantial run-down after patch excision. The cells were exposed to symmetrical $[K^+]$ at a nominal $[Ca^{2+}]_i$ of 0.3 µM and currents at -75 mV were plotted as a function of time. Fig. 2A shows that GW542573X enhanced the hSK1 current in a concentration-dependent manner when applied to the extracellular solution at concentrations ranging from 0.1 to 10 µM. At the beginning of the experiment 0.1 µM NS309 was added as a control and the experiment was terminated by addition of the fast SK channel blocker bicuculline methobromide (BMB, 300 µM). Fig. 2B-D show data from HEK293 cells expressing hSK2 (B), hSK3 (C) or hIK (D, experiment terminated by 30 nM charybdotoxin, ChTX). Fig. 2E summarizes the results from these experiments. The fold increase in current levels induced by NS309 was not statistically different between the SK subtypes (hSK1: 5.99 ± 0.56; hSK2: 6.28 ± 0.91; hSK3: 6.33 ± 0.51), whereas the enhancement of the hIK current level was more prominent (15.56 ± 1.96 fold stimulation, $P < 0.001$, one way ANOVA). In contrast, GW542573X was a more potent modulator of hSK1 than of hSK2, hSK3 or hIK channels at all concentrations tested. GW542573X induced no effects at the hSK2, hSK3 or hIK current level at 0.1 and 1 µM, but hSK2 and hSK3 currents were increased at 10 µM GW542573X to a similar degree that was higher than the response obtained for the hIK current ($P < 0.001$, one way ANOVA). Whilst we have not done

Molecular Pharmacology Fast Forward. Published on June 10, 2009 as DOI: 10.1124/mol.109.056663
This article has not been copyedited and formatted. The final version may differ from this version.

an exhaustive analysis of activity across other channel and receptor types, GW542573X produced < 10% inhibition at 30 μM *vs* representative voltage-gated Na^+ ($Na_v1.3$), Ca^{2+} ($Ca_v2.2$) and K^+ channels ($K_v1.3$), as well as exemplar ligand gated ion channels (P2X2/3, nicotinic α7). Thus GW542573X is an SK1-selective activator.

We next investigated whether GW542573X acted as a "classical" positive modulator of hSK1. The hitherto known positive modulators increase the apparent Ca^{2+}-sensitivity of SK channels, a property reflected in a leftward shift in the Ca^{2+}-response curve (Pedarzani et al., 2001; Hougaard et al., 2007). The effect of GW542573X on the Ca^{2+}-response relationship of hSK1 is elucidated in Fig. 3A using inside-out patches. The patch was exposed first to 0.01 μM Ca^{2+} to determine the background current level and subsequently to 10 μM Ca^{2+} to define the maximal current. After re-exposure to 0.01 μM Ca^{2+}, the $[Ca^{2+}]_i$ in the intracellular solution was increased in a step-wise manner with GW542573X present as shown by the bar. Note the clear activation at 0.01 μM Ca^{2+} as well as the drop in current upon compound wash-out at 10 μM Ca^{2+}. In Fig. 3B the effect of 10 μM GW542573X on the Ca^{2+}-response relationship of hSK1 is presented. GW542573X induced a leftward shift in the apparent Ca^{2+}-dependence, reducing the EC_{50} value for Ca^{2+} from 410 ± 20 nM (n = 9) to 240 ± 10 nM (n = 5, $p < 0.01$ students *t*-test). In addition, GW542573X also increased the maximal degree of hSK1 channel activation as evidenced by an increased current level at saturating Ca^{2+} concentration (I/Imax > 1). Interestingly, a small (4.0 ± 0.8 % of the maximal current, n = 5) but reproducible and significant increase in current was also observed at very low Ca^{2+} concentrations. In contrast to GW542573X, NS309 only induces a leftward shift in the Ca^{2+}-response

Molecular Pharmacology Fast Forward. Published on June 10, 2009 as DOI: 10.1124/mol.109.056663
This article has not been copyedited and formatted. The final version may differ from this version.

relationship, reducing the EC_{50} value for Ca^{2+} to 140 ± 20 nM (n = 3) without affecting the current level at the very low or saturating Ca^{2+} concentrations.

The complex effects of GW542573X on the Ca^{2+}-response relationship of hSK1 prompted a more detailed study of GW542573X at different $[Ca^{2+}]_i$ and a comparison to the hSK1 current enhancement induced by the more "classical" positive modulator NS309. Fig. 4A shows the time course of an experiment where 10 µM GW542573X was tested at nominally 0, 0.2 or 10 µM intracellular Ca^{2+} and Fig. 4B shows the corresponding IV relationships. GW542573X induced a small but distinct increase in the current level in the absence of Ca^{2+} and the IV relationship shifted from being linear (reflecting non-specific leak current) to exhibiting the characteristic inward rectification typical for SK channels recorded under these conditions. At the intermediate Ca^{2+} concentration, GW542573X produced a prominent stimulation of the current (from 5% (Ctrl) to 60% of full Ca^{2+} activation) and at the saturating Ca^{2+} concentration, GW542573X enhanced the current by approximately 15%. Both at the intermediate and at the high Ca^{2+} concentrations the current stimulated by GW542573X maintained the typical inward rectification. Fig. 4C&D show results from a similar experiment conducted with 1 µM NS309. Unlike GW542573X, NS309 was unable to stimulate the current at 0 or 10 µM Ca^{2+} whereas a substantial potentiation of the current was observed at 0.2 µM Ca^{2+} (from 8% (Ctrl) to 90% of full activation).

The rather surprising observation that GW542573X is not just a positive modulator, but is, in fact, also able to activate hSK1 Ca^{2+}-independently led us to investigate whether the GW542573X-activated hSK1 channel, like the Ca^{2+}-activated, was sensitive to the SK channel blocker apamin and to positive modulation by NS309. Fig. 5A shows the time course of a whole-cell experiment with zero added Ca^{2+} and

Molecular Pharmacology Fast Forward. Published on June 10, 2009 as DOI: 10.1124/mol.109.056663
This article has not been copyedited and formatted. The final version may differ from this version.

10 mM of EGTA in the pipette solution. The whole-cell configuration was chosen for this purpose since, 1) apamin is unable to block SK channels when applied from the intracellular side of the membrane and 2) GW542573X-induced activation at zero Ca^{2+} only amounts to about 4 % of the maximal current, which is considered too low for reliable assessment of additional pharmacological modulation. The letters a-d indicate the time points where the IV relationships shown in Fig. 5B were obtained. First, the cell was exposed to 10 μM NS309 (a) that did not induce any increase in control current (b) suggesting that under these experimental conditions $[Ca^{2+}]_i$ was too low (well below 10 nM, see Hougaard et al, 2007) to sustain NS309-mediated hSK1 activation. A subsequent application of 10 μM GW542573X (c) resulted in a robust stimulation of a current (1.6 ± 0.3 nA, n = 11), which was sensitive to inhibition by apamin (200 nM, d). We then tested whether the GW542573X-activated channel was sensitive to positive modulation (Fig. 5C&D). Although 10 μM NS309 (d) alone was unable to activate hSK1 channels in the absence of added Ca^{2+} it could further enhance (by 0.7 ± 0.2 nA, n = 6) (c) the hSK1 current activated by GW542573X (b) suggesting a synergistic or an additive action of GW542573X and NS309 at the hSK1 channel level. Similar effects were observed with a classic SK channel modulator from another chemical class (a riluzole analogue, data not shown).

Based on experiments with IK/SK2 chimeras, Pedarzani and co-workers (Pedarzani et al., 2001) showed that 1-EBIO mediated its stimulating effect via the C-terminal of the channels. Using hSK1-hSK3 chimeras, we have previously reported that amino acids within, and just distal to the CAMBD is responsible for the SK3/2-selective channel modulation by CyPPA (Hougaard et al., 2008). A similar approach was adopted to identify the channel regions important for the selectivity of GW542573X for SK1 over SK3. We focused on the SK subtype selectivity rather

Molecular Pharmacology Fast Forward. Published on June 10, 2009 as DOI: 10.1124/mol.109.056663
This article has not been copyedited and formatted. The final version may differ from this version.

than on the more pronounced SK1-IK selectivity, based on the assumption that chimeras from the nearly identical SK-channels would most likely reflect genuine SK channel pharmacological properties. However, preliminary experiments were conducted with SK1-IK chimeras (including C-terminal switch, data not shown) yielding confirmative information to the more refined analysis outlined below. All chimeras were screened using whole-cell experiments on transiently transfected HEK293 cells. NS309 (30 nM) was applied at the beginning of the experiments to ensure that the chimeras had retained normal sensitivity to positive modulation. After wash-out of NS309, 200 nM GW542573X was applied, since this concentration induced a potentiation of SK1 channels of similar amplitude as 30 nM NS309, while having no effect on SK3. The overall topology of the chimeras and the results from this screening are presented in Fig. 6A; furthermore an alignment showing the exact point mutations is presented in Fig. 6B.

Initially, two hSK1-hSK3 chimeras were generated addressing the roles of the N-terminal plus the transmembrane regions *vs* the C-terminal harboring the CaMBD. Chimera 1 represents an hSK3 channel with an hSK1 C-terminal and whole-cell experiments showed that insertion of the hSK1 C-terminal did not enable modulation by GW542473X. Consistently, introduction of an SK3 C-terminal into hSK1 as for Chimera 2 did not eliminate the effect of GW542573X. Chimera 1 and 2 were characterized further and Fig. 7A&B show that whereas 1 μM GW542573X induced an increase in current mediated by Chimera 2, 10 μM GW542573X was required to modulate Chimera 1, demonstrating that the SK1-selective modulation by GW542573X is dependent on the N-terminal and/or the transmembrane regions. Comparison of panel B in Fig. 7 with panel C in Fig. 2 shows furthermore that the

Molecular Pharmacology Fast Forward. Published on June 10, 2009 as DOI: 10.1124/mol.109.056663
This article has not been copyedited and formatted. The final version may differ from this version.

response of Chimera 2 to GW542573X was not different from that of wild type SK1, whereas Chimera 1 was hSK3-like in the response to GW542573X.

To address specifically the role of the N-terminal domain and the intracellular loop between S2 and S3, Chimera 3 was generated and GW542573X induced an increase in current similar to that on hSK1. Furthermore, testing Chimera 4, which is SK1 only in S3-S6, elucidated that determinants of SK1-selective modulation are located in transmembrane regions surrounding the pore. Five regions within S3-S5 were point mutated (Chimeras 5-9), walking from S3 to S5, exchanging only hSK1 amino acids being different from both hSK2 and hSK3 to their equivalent hSK3 amino acids. Chimeras 5-8 were all hSK1-like in their responses to GW542573X. However, Chimera 9 exhibited an increase of only 1.09 ± 0.04, indicating relative insensitivity to GW542573X. The only difference between Chimera 3 and Chimera 9 is the introduction of a serine residue in position 293, thus this amino acid appears to play a critical role for the sensitivity towards GW542573X.

A leucine residue is present in both hSK2 and hSK3 at the equivalent position of the hSK1S293. This leucine residue (L476 in hSK3) was mutated to a serine residue in hSK3 resulting in $hSK3_{L476S}$ (Chimera 10), being a GW542573X-sensitive channel. Chimera 10 was further investigated in whole-cell experiments (Fig. 7C) in a similar protocol as used for Chimera 1 and 2. Evidently, this single amino acid substitution in hSK3 fully mimicked the potency of GW542573X on Chimera 2 and hence also on hSK1 (compare with Fig. 7B and Fig. 2A). Fig. 7D summarizes the concentration responses of GW542573X on Chimera 1, 2 and 10 ($hSK3_{L476S}$) bracketed by the concentration responses on the hSK1 and hSK3 wild types.

Finally, Fig. 8A shows concentration-response relationships of GW542573X performed on inside-out patches with hSK3 and Chimera 10 ($hSK3_{L476S}$). Whereas

Molecular Pharmacology Fast Forward. Published on June 10, 2009 as DOI: 10.1124/mol.109.056663
This article has not been copyedited and formatted. The final version may differ from this version.

GW542573X barely stimulated the hSK3 current in concentrations up to 50 μM, substantial activation of $hSK3_{L476S}$ was seen. Fitting these data to the Hill equation yielded EC_{50} values of 9.3 ± 1.4 μM (n = 5) which is not significantly different from that estimated for the hSK1 (8.2 ± 0.8 μM, n = 6, dashed curve) and in good agreement with the whole-cell data shown in Fig. 7. The only difference between $hSK3_{L476S}$ and hSK1 was an apparent slightly lower efficacy of GW542573X on $hSK3_{L476S}$ (50 ± 7%, n = 5) compared to hSK1 (76 ± 5%, n = 6). Finally, in order to investigate whether S293 also accounted for the new MOA of GW542573X, we tested the ability of the compound to activate $hSK3_{L476S}$ in the absence of intracellular Ca^{2+}. As seen from the whole-cell data in Fig. 8B GW542573X is, in contrast to NS309, able to activate $hSK3_{L476S}$ Ca^{2+}-independently, similar to what is observed for hSK1 wild-type channels.

Thus, we conclude that the serine residue at position 293 in hSK1 essentially account for the selective activation of SK1 and most likely also for the novel MOA described here for GW542573X. This shows that S293 positioned in S5 at a position closely opposed to the pore region constitute an important site for modulation of the gating process of SK channels.

Molecular Pharmacology Fast Forward. Published on June 10, 2009 as DOI: 10.1124/mol.109.056663
This article has not been copyedited and formatted. The final version may differ from this version.

Discussion

In this paper we present a new chemical substance, GW542573X, characterized as a selective activator of human SK channels. The compound is structurally unrelated to previously described compounds in this pharmacological category: 1-EBIO, DC-EBIO, riluzole, SKA-31 and NS309 having limited SK subtype selectivity and higher affinity for IK channels (IK>SK1=SK2=SK3), and the selective SK3/SK2 modulator CyPPA (SK3>SK2>>SK1=IK). GW542573X exhibits a novel selectivity profile being selective for SK1 over SK2/SK3 and essentially inactive on IK (SK1>SK2=SK3>IK). From a selectivity point-of-view GW542573X is therefore complementary to CyPPA and these compounds (or more potent congeners) have the potential to be useful tools for investigations aimed at defining the physiological roles of the SK channel subtypes, including the poorly defined function of SK1. However, since the rat SK1 isoform does not express in cell lines, possible species differences in the pharmacology of SK channels remain a caveat for such studies.

Importantly, the MOA of GW542573X also is unique. Previously published compounds all induce a leftward shift of the $[Ca^{2+}]_i$ response curves without activating at low $[Ca^{2+}]_i$ where the channel open state probability is zero, or augmenting at high $[Ca^{2+}]_i$ where the channel is maximally activated (open state probability ≈ 80 %, (Hirschberg et al., 1998)). In contrast, GW542573X causes a (minor) leftward shift in the $[Ca^{2+}]_i$ response curve for SK1, but additionally causes a partial activation in the absence of $[Ca^{2+}]_i$ and furthermore increases the current level achievable at saturating $[Ca^{2+}]_i$. GW542573X is thus able to partially uncouple SK1 channel activation from the physiological ligand. Since the activation occurs swiftly upon application to completely closed channels, we hypothesize that the molecular mechanism relates to destabilization of a closed state rather than to stabilization of an

Molecular Pharmacology Fast Forward. Published on June 10, 2009 as DOI: 10.1124/mol.109.056663
This article has not been copyedited and formatted. The final version may differ from this version.

open state. The additive effect observed at a $[Ca^{2+}]_i$ too low for NS309 to activate SK1 by itself probably represents the polar opposite effect (open channel stabilization), thereby pinpointing another fundamental difference between GW542573X and the hitherto known positive modulators.

The unusual selectivity profile and MOA is independent of the CaMBD in the C-terminal, which is essential for the positive modulation by 1-EBIO (Pedarzani et al., 2001) and CyPPA (Hougaard et al., 2008). Rather, both the selectivity profile and the special MOA are tightly linked to a single amino acid, S293 located in S5 at the level of the inner pore vestibule just below the ion selectivity filter. This conclusion was obtained from the hSK3/hSK1 chimera approach using the non-discriminating NS309 as a control for preserved "normal SK activator pharmacology" of the various chimeras, thereby gradually homing in on domains important for the selectivity of GW542573X. Eventually the point mutation L476S in hSK3 (the position equivalent to S293 in hSK1), was identified as the substitution that can restore the functional potency of GW542573X to the same extent as observed for hSK1. It is important to note, however, that while this point mutation fully accounts for the selectivity pattern among the SK channels (hSK2 express L321) additional determinants must participate in the even more pronounced selectivity against hIK (which express the equivalent L215). Since the S293 in hSK1 is conserved in the rat isoform it is anticipated that GW542573X will be preferentially active on rSK1 over rSK2, rSK3 and rIK as well.

These experiments show for the first time that gating properties of SK channels can be influenced by interaction with amino acids in transmembrane regions close to the inner pore vestibule and the selectivity filter. The results may be interesting, not only from a pharmacological perspective defining a new site of action, but also in relation to the ongoing debate on the nature and position of the natural

Molecular Pharmacology Fast Forward. Published on June 10, 2009 as DOI: 10.1124/mol.109.056663
This article has not been copyedited and formatted. The final version may differ from this version.

gating process of SK/IK channels: Upon binding of Ca^{2+} at the N-lobes of the attached CaM, a conformational change in the CaM/CaMBD (Schumacher et al., 2001) induces an intramolecular gating cascade that is transmitted by the CaMBD-S6 linker via S6 to a structure in or close to the selectivity filter, which constitutes the physical gate. This conclusion is based on a series of papers with SK2 channels, where substituted cysteine accessibility scans were performed from the proximal CaM/CaMBD-S6 linker along the S6 deep into the pore. The main conclusion reached from these experiments (Bruening-Wright et al., 2002; Bruening-Wright et al., 2007), is that the equivalent position to the classical S6 "bundle crossing" at the intracellular end of K_v channels, does not exclude even bulky reducing agents like $MTSEA^+$ from acting at "deep pore" positions like A384C in SK2 channels, even when the channel is closed by low $[Ca^{2+}]_i$. On the other hand Ba^{2+}, a K^+-analog, that specifically binds at the selectivity filter and blocks the current of K^+ through SK channels only in the open state, prevents $MTSEA^+$ modification at A384, indicating that the gate and the selectivity filter may be functionally connected. A similar experimental strategy was also adopted for the IK channel (Klein et al., 2007; Garneau et al., 2008), clearly revealing that V275, which is equivalent to A384 in SK2, is accessible in the closed state for reduction by Ag^+, a K^+ sized ion. Very interestingly, this study also showed that mutations at specific hydrophobic amino acids (A279G, V282G in IK, V391G in SK2) in the pore region lead to constitutively active channels being insensitive towards $[Ca^{2+}]_i$. This finding suggests hydrophobic interactions of S6 as being essential for the stabilization of the gate in the closed conformation and furthermore that transmission of the CaM-Ca^{2+} gating signal to the gate most likely involves an exposure of the hydrophobic V282 to water.

Assuming that the actions of GW542573X shown in the present study are influencing the physiological "gating machinery" of SK channels (although twisting it away from normal physiological function!) it is tempting to assume that the compound interacts with gating structures residing deep in the inner pore vestibule possibly close to the selectivity filter. Thereby these data may be an independent pharmacological support of the concept of deep pore gating in SK channels. While the above mentioned attempts to localize the gate by cysteine scanning has exclusively been directed at the most likely "transduction pathway" between the CaMBD and the gate - the S6 - the present study pinpoints amino acids in S5 as being close enough to central gating mechanisms to influence the process. S5 amino acids in this region are not lining the pore vestibule in the potassium channel structures solved so far and not depicted as such in SK/IK homology models. Hence it is unlikely that S293 acts as a "gating particle" *per se*, whereas it may well serve a stabilizing function for the closed channel, possibly by interhelical S5-S6 interactions. We cannot, however, distinguish between S273 being an important determinant of natural gating of SK1 or if it rather constitutes a favorable coordination site for GW542573X, which then by itself interferes with critical amino acid interactions important for stabilization of the closed conformation.

Conclusion and perspective

Classical IK/SK channel openers (1-EBIO, CyPPA, and probably SKA-31 and NS309 as well), act via the CaM/CaMBD at the C-terminal. These compounds exclusively activate SK channels by increasing the apparent affinity for Ca^{2+} and can be formally categorized as positive allosteric modulators. In contrast, GW542573X acts via S293 in S5 possibly at a site near the physical gate thereby influencing gating processes

Molecular Pharmacology Fast Forward. Published on June 10, 2009 as DOI: 10.1124/mol.109.056663
This article has not been copyedited and formatted. The final version may differ from this version.

seemingly intercalated between Ca^{2+}-binding and channel opening. GW542573X partially "bypasses" the physiological activating signal and is therefore best described as a partial agonist of hSK1 channels. In our view, GW542573X represents primarily an *in vitro* tool for research aimed at elucidating the gating process in SK channels. Secondary, it may delineate a route towards the synthesis of SK1-selective agents with higher potency and stability that may also be useful in the establishment of the – still obscure – physiological/pathological relevance of SK1 in the brain.

Acknowledgements

The authors gratefully acknowledge the help from Lene Gylle Larsen with the molecular biology, Anne Stryhn Meincke with the patch clamp experiments, Sandra Arpino and Melanie Armstrong with the VIPR assays, Graeme Robertson and Matthew Crowe with the medicinal chemistry and Nicoletta Garbati for input into the early chimera work.

References

Allen D, Fakler B, Maylie J, and Adelman JP (2007) Organization and regulation of small conductance Ca^{2+}-activated K^+ channel multiprotein complexes. *J Neurosci* **27:**2369-2376.

Bildl W, Strassmaier T, Thurm H, Andersen J, Eble S, Oliver D, Knipper M, Mann M, Schulte U, Adelman JP, and Fakler B (2004) Protein kinase CK2 is coassembled with small conductance Ca^{2+}-activated K^+ channels and regulates channel gating. *Neuron* **43:**847-858.

Bond CT, Maylie J, and Adelman JP (2005) SK channels in excitability, pacemaking and synaptic integration. *Curr Opin Neurobiol* **15:**305-311.

Bruening-Wright A, Lee WS, Adelman JP, and Maylie J (2007) Evidence for a deep pore activation gate in small conductance Ca^{2+}-activated K^+ channels. *J Gen Physiol* **130:**601-610.

Bruening-Wright A, Schumacher MA, Adelman JP, and Maylie J (2002) Localization of the activation gate for small conductance Ca^{2+}-activated K^+ channels. *J Neurosci* **22:**6499-6506.

Dale TJ, Cryan JE, Chen MX, and Trezise DJ (2002) Partial apamin sensitivity of human small conductance Ca^{2+}-activated K^+ channels stably expressed in Chinese hamster ovary cells. *Naunyn Schmiedebergs Arch Pharmacol* **366:**470-477.

Desai R, Peretz A, Idelson H, Lazarovici P, and Attali B (2000) Ca^{2+}-activated K^+ channels in human leukemic Jurkat T cells. Molecular cloning, biochemical and functional characterization. *J Biol Chem* **275:**39954-39963.

Garneau L, Klein H, Banderali U, Longpré-Lauzon A, Parent L, and Sauvé R (2008) Hydrophobic interactions as key determinants to the KCa3.1 channel closed configuration: An analysis of KCa3.1 mutants constitutively active in zero Ca^{2+}. *J Biol Chem* **284:**389-403.

González JE, Oades K, Leychkis Y, Harootunian A, and Negulescu PA (1999) Cell-based assays and instrumentation for screening ion channel targets. *Drug Discov Today* **4:** 431-439.

Hirschberg B, Maylie J, Adelman JP, and Marrion NV (1998) Gating of recombinant small-conductance Ca-activated K^+ channels by calcium. *J Gen Physiol* **111:**565-581.

Hougaard C, Eriksen BL, Jørgensen S, Johansen TH, Dyhring T, Madsen LS, Strøbæk D, and Christophersen P (2007) Selective positive modulation of the SK3 and SK2 subtypes of small conductance Ca^{2+}-activated K^+ channels. *Br J Pharmacol* **151:**655-665.

Hougaard C, Jensen ML, Hummel R, Johansen TH, Eriksen BL, Strøbæk D, and Christophersen P (2008) Positive modulation by the SK2/SK3-selective compound, CyPPA, is mediated via the C-terminal tail. *Biophys J* **94:**2199.

Jensen BS, Strøbæk D, Christophersen P, Jørgensen TD, Hansen C, Silahtaroglu A, Olesen SP, and Ahring PK (1998) Characterization of the cloned human intermediate-conductance Ca^{2+}-activated K^+ channel. *Am J Physiol* **275:**C848-856.

Khanna R, Chang MC, Joiner WJ, Kaczmarek LK, and Schlichter LC (1999) hSK4/hIK1, a calmodulin-binding K_{Ca} channel in human T lymphocytes. Roles in proliferation and volume regulation. *J Biol Chem* **274:**14838-14849.

Klein H, Garneau L, Banderali U, Simoes M, Parent L, and Sauvé R (2007) Structural determinants of the closed KCa3.1 channel pore in relation to channel gating:

results from a substituted cysteine accessibility analysis. *J Gen Physiol* **129:**299-315.

Köhler M, Hirschberg B, Bond CT, Kinzie JM, Marrion NV, Maylie J, and Adelman JP (1996) Small-conductance, calcium-activated potassium channels from mammalian brain. *Science* **273:**1709-1714.

Maingret F, Coste B, Hao J, Giamarchi A, Allen D, Crest M, Litchfield DW, Adelman JP, and Delmas P (2008) Neurotransmitter modulation of small-conductance Ca^{2+}-activated K^+ channels by regulation of Ca^{2+} gating. *Neuron* **59:**439-449.

Martina M, Turcotte ME, Halman S, and Bergeron R (2007) The sigma-1 receptor modulates NMDA receptor synaptic transmission and plasticity via SK channels in rat hippocampus. *J Physiol* **578:**143-157.

Pedarzani P, Mosbacher J, Rivard A, Cingolani LA, Oliver D, Stocker M, Adelman JP, and Fakler B (2001) Control of electrical activity in central neurons by modulating the gating of small conductance Ca^{2+}-activated K^+ channels. *J Biol Chem* **276:**9762-9769.

Pedarzani P and Stocker M (2008) Molecular and cellular basis of small- and intermediate-conductance, calcium-activated potassium channel function in the brain. *Cell Mol Life Sci* **65:**3196-3217.

Sankaranarayanan A, Raman G, Busch C, Schultz T, Zimin PI, Hoyer J, Köhler R, and Wulff H (2009) Naphtho[1,2-*d*]thiazol-2-ylamine (SKA-31), a new activator of KCa2 and KCa3.1 potassium channels, potentiates the EDHF response and lowers blood pressure. *Mol Pharmacol* **75:**281-295.

Schumacher MA, Rivard AF, Bächinger HP, and Adelman JP (2001) Structure of the gating domain of a Ca^{2+}-activated K^+ channel complexed with Ca^{2+}/calmodulin. *Nature* **410:**1120-1124.

Stocker M (2004) Ca^{2+}-activated K^+ channels: molecular determinants and function of the SK family. *Nat Rev Neurosci* **5:**758-770.

Strøbæk D, Hougaard C, Johansen TH, Sørensen US, Nielsen EØ, Nielsen KS, Taylor RD, Pedarzani P, and Christophersen P (2006) Inhibitory gating modulation of small conductance Ca^{2+}-activated K^+ channels by the synthetic compound (R)-N-(benzimidazol-2-yl)-1,2,3,4-tetrahydro-1-naphtylamine (NS8593) reduces afterhyperpolarizing current in hippocampal CA1 neurons. *Mol Pharmacol* **70:**1771-1782.

Strøbæk D, Jørgensen TD, Christophersen P, Ahring PK, and Olesen SP (2000) Pharmacological characterization of small-conductance Ca^{2+}-activated K^+ channels stably expressed in HEK 293 cells. *Br J Pharmacol* **129:**991-999.

Strøbæk D, Teuber L, Jørgensen TD, Ahring PK, Kjær K, Hansen RS, Olesen SP, Christophersen P, and Skaaning-Jensen B (2004) Activation of human IK and SK Ca^{2+}-activated K^+ channels by NS309 (6,7-dichloro-1H-indole-2,3-dione 3-oxime). *Biochim Biophys Acta* **1665:**1-5.

Sørensen US, Strøbæk D, Christophersen P, Hougaard C, Jensen ML, Nielsen EØ, Peters D, and Teuber L (2008) Synthesis and structure-activity relationship studies of 2-(N-Substituted)-aminobenzimidazoles as potent negative gating modulators of small conductance Ca^{2+}-activated K^+ Channels. *J Med Chem* **51:**7625-7634.

Xia XM, Fakler B, Rivard A, Wayman G, Johnson-Pais T, Keen JE, Ishii T, Hirschberg B, Bond CT, Lutsenko S, Maylie J, and Adelman JP (1998) Mechanism of calcium gating in small-conductance calcium-activated potassium channels. *Nature* **395:**503-507.

Molecular Pharmacology Fast Forward. Published on June 10, 2009 as DOI: 10.1124/mol.109.056663
This article has not been copyedited and formatted. The final version may differ from this version.

Legends for Figures

Fig. 1

GW542573X, a new positive modulator of SK channels

(**A**) Chemical structure of GW542573X. (**B**) VIPR membrane potential measurements from hSK1 expressing cells in the absence (0) and presence of increasing concentrations (0.38-100 μM) of GW542573X. The abscissa shows time and the solid bar the duration of the compound application. The ordinate shows the calculated Rf/Ri values which reduce in size upon membrane hyperpolarisation. (**C**) Representative concentration-response curve for GW542573X evoked peak changes in membrane potential. The derived EC_{50} value from the fit to the Hill-equation was 3.1 μM with a n_H value of 0.96. (**D**) An inside-out patch obtained from a HEK293 cell stably expressing hSK1. The patch was exposed to symmetrical [K^+] (154 mM) and 200 ms voltage ramps (-80 to +80 mV) were elicited every 5 s from a holding potential of 0 mV. The solid lines are IV relationships obtained at a bath/intracellular [Ca^{2+}] of 0.2 or 10 μM in the absence of GW542573X, whereas the dotted lines represent IV relationships in the presence of GW542573X (0.2 μM Ca^{2+}, [GW542573X] from 0.1 to 50 μM as indicated). (**E**) Concentration-response relationship for GW542573X performed in the presence of 0.2 μM Ca^{2+}. Currents were normalized with respect to the effect of 10 μM Ca^{2+}, which induces maximal SK channel activity, and data points represent mean ± S.E.M. of 6 experiments. Data was analyzed at -75 mV. The solid line is the fit of the averaged data to the Hill equation yielding an EC_{50} value of 7.8 μM and a n_H value of 1.4. The efficacy was 72%.

Molecular Pharmacology Fast Forward. Published on June 10, 2009 as DOI: 10.1124/mol.109.056663
This article has not been copyedited and formatted. The final version may differ from this version.

Fig. 2

GW542573X is an SK1–selective activator

Whole-cell currents recorded from HEK293 cells stably expressing hSK1 (**A**), hSK2 (**B**), hSK3 (**C**) or hIK (**D**). The pipette [Ca^{2+}] was buffered at 0.3 µM. The voltage protocol was as described in the legend to Fig. 1 and current recorded at -75 mV is plotted as a function of time. NS309 (0.1 µM) or GW542573X (0.1, 1 or 10 µM) were added to the bath solution as indicated by the bars. The experiments were terminated by the addition of 300 µM bicuculline methobromide (BMB, SK experiments) or 30 nM charybdotoxin (ChTX, IK experiments). (**E**) Average currents (mean ± S.E.M.) in the presence of GW542573X (0.1, 1 or 10 µM) or NS309 (0.1 µM). Currents in the presence of compound are shown relative to the SK/IK current level just prior to compound addition (indicated by the dashed line) (n = 4 - 5).

Fig. 3

GW542573X exerts complex effects on the Ca^{2+} concentration-response relationship of SK1

(**A**) hSK1 current (inside-out patch) measured at -75 mV and depicted as a function of time. The [Ca^{2+}] in the bath/intracellular solution was increased from 0.01 to 10 µM in a step-wise manner as indicated on the abscissa and 10 µM GW542573X was present as shown by the bar. (**B**) Ca^{2+}-response curves, obtained from experiments similar to the one depicted in (**A**) either in the absence (Ctrl) or presence of 10 µM GW542573X or 1 µM NS309. Currents from individual patches were normalized with respect to the effect of 10 µM Ca^{2+}. Data points are mean ± S.E.M. of 9

Molecular Pharmacology Fast Forward. Published on June 10, 2009 as DOI: 10.1124/mol.109.056663
This article has not been copyedited and formatted. The final version may differ from this version.

experiments under control conditions, 5 experiments in the presence of GW542573X, and 3 in the presence of NS309. The solid lines are the fit of data to the Hill equation. Note that in the presence of GW542573X, the efficacy with respect to 10 μM Ca^{2+} without compound was 117%, and that a small increase in current was induced by the compound at the very low [Ca^{2+}].

Fig. 4

GW542573X is not just a positive modulator but also an SK channel opener

(**A**) hSK1 current at -75 mV depicted as a function of time. Current was measured from an inside-out patch obtained from a HEK293 cell stably expressing hSK1. The patch was exposed to 10 μM GW542573X either in the complete absence of Ca^{2+} (0) or at 0.2 or 10 μM intracellular Ca^{2+}. (**B**) I-V relationships at 0, 0.2 or 10 μM Ca^{2+} in the absence (Ctrl) or presence of 10 μM GW542573X as indicated. (**C&D**) similar experiment as in (**A&B**)**,** but with NS309 (1 μM) instead of GW542573X (n = 3 – 5).

Fig. 5

The SK current activation by GW542573X in the absence of Ca^{2+} is sensitive to positive modulation and block

(**A&C**) Whole-cell hSK1 current at -75 mV depicted as a function of time. The [Ca^{2+}] in the pipette solution was below 1 nM (no added Ca^{2+} and 10 mM EGTA). NS309 (10 μM), GW542573X (10 μM) and the SK channel blocker Apamin (200 nM) were added to the perfusate as shown by the bars. (**B&D**) Whole-cell IV relationships measured at the time points indicated by letters in (**A&C**). Data are from single experiments, and are representative of 5-6 independent observations.

Molecular Pharmacology Fast Forward. Published on June 10, 2009 as DOI: 10.1124/mol.109.056663
This article has not been copyedited and formatted. The final version may differ from this version.

Fig. 6

Identification of the amino acid important for functional effects of GW542573X on hSK1 via effects on chimera and point mutated channels

(**A**) Effects of NS309 and GW542573X on wild type hSK1 and hSK3 and various channel chimeras. Regions shown in gray indicate hSK1 domains and regions shown in black are from hSK3. Fold increase in whole-cell current in the presence of 30 nM NS309 and in the presence 200 nM GW542573X is given for each channel as mean ± S.E.M. GW542573X current increase normalized to NS309 is calculated as (fold increase GW542573X)/(fold increase NS309) for each cell and is shown graphically as mean ± S.E.M. Vertical lines represents values for wt hSK1 (dashed) and wt hSK3 (solid). (**B**) Amino acid alignment of hSK1 and hSK3. S3, S4 and S5 are indicated as black lines above the alignment and mutated amino acids are indicated by stars for chimeras 5-9.

Fig. 7

The effect of GW542573X is mainly conferred by parts upstream the C-terminus

(**A - C**) Whole-cell currents recorded from HEK293 cells expressing Chimera 1 (**A**), Chimera 2 (**B**) or Chimera 10 ($hSK3_{L476S}$, **C**). Currents were recorded at -75 mV and plotted as a function of time. NS309 (0.1 µM) or GW542573X (0.1, 1 or 10 µM) were added to the bath solution as indicated by the bars. The $[Ca^{2+}]_i$ was 0.3 µM and the experiments were terminated by the addition of 300 µM BMB. (**D**) Current (mean ± S.E.M.) in the presence of GW542573X (0.1, 1 or 10 µM) or NS309 (0.1 µM). For illustrative purposes data on SK1 and SK3, previously presented in Fig. 2, is included.

Molecular Pharmacology Fast Forward. Published on June 10, 2009 as DOI: 10.1124/mol.109.056663
This article has not been copyedited and formatted. The final version may differ from this version.

Currents in the presence of compound are shown relative to the SK current level just prior to compound addition (indicated by the dashed line) (n = 4 - 5).

Fig. 8

Exchanging leucine in position 476 of hSK3 with the corresponding serine in hSK1 makes the channel SK1-like in the response towards GW542573X

(**A)** Concentration-response relationship of GW542573X on $hSK3_{L476S}$ and hSK3 channels measured on inside-out patches. Currents were normalized with respect to the effect of 10 µM Ca^{2+} and data points represent mean ± S.E.M. of 5 experiments both for hSK3 and $hSK3_{L476S}$ channels. The solid lines are the fit of the averaged data to the Hill equation. For comparison the data obtained on hSK1 (from Fig. 1) is shown as a dashed line. (**B**) Whole-cell current from a cell transfected with $hSK3_{L476S}$ channels depicted as a function of time. The [Ca^{2+}] in the pipette solution was below 1 nM (no added Ca^{2+} and 10 mM EGTA). GW542573X (10 µM) and NS309 (10 µM) were added to the perfusate as shown by bars.

Figure 1

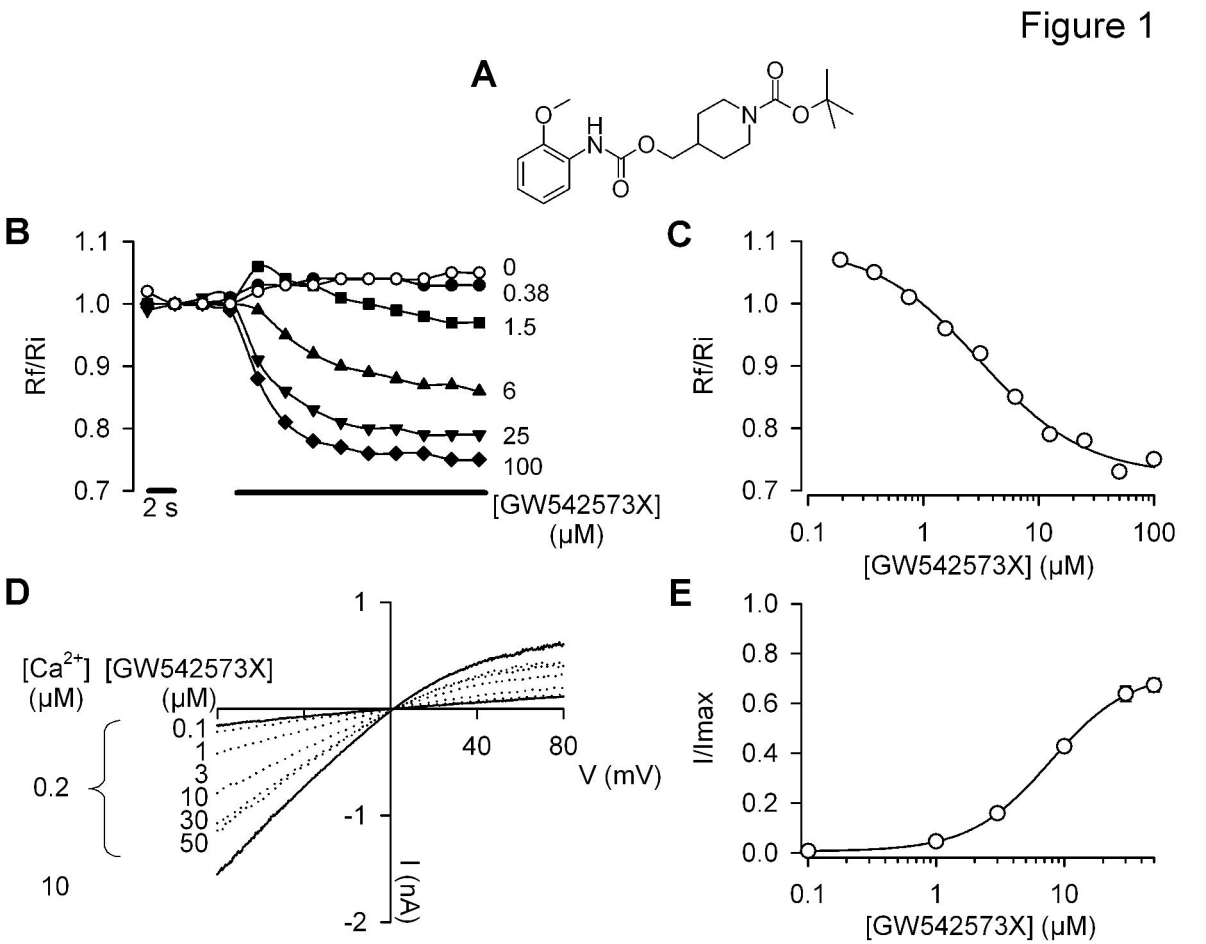
A
B
1.1
1.0
0.9
0.8
0.7
Rf/Ri
0
0.38
1.5
6
25
100
2 s
[GW542573X]
(μM)
C
1.1
1.0
0.9
0.8
0.7
Rf/Ri
0.1
1
10
100
[GW542573X] (μM)
D
[Ca2+]
(μM)
[GW542573X]
(μM)
0.2
10
0.1
1
3
10
30
50
1
-1
-2
40
80
V (mV)
I (nA)
E
1.0
0.8
0.6
0.4
0.2
0.0
I/Imax
0.1
1
10
[GW542573X] (μM)

Figure 2

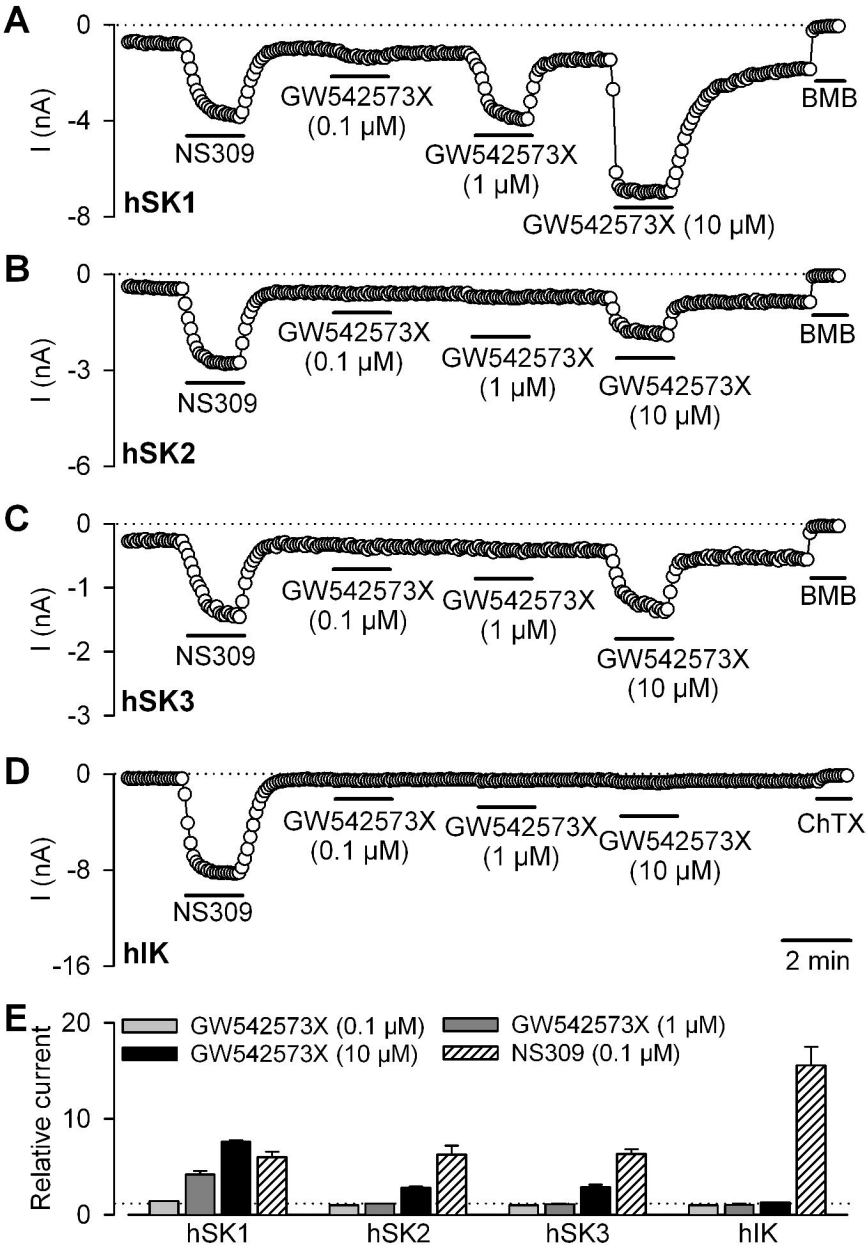
A
0
-4
-8
I (nA)
NS309
GW542573X (0.1 μM)
GW542573X (1 μM)
GW542573X (10 μM)
BMB
hSK1
B
0
-3
-6
I (nA)
NS309
GW542573X (0.1 μM)
GW542573X (1 μM)
GW542573X (10 μM)
BMB
hSK2
C
0
-1
-2
-3
I (nA)
NS309
GW542573X (0.1 μM)
GW542573X (1 μM)
GW542573X (10 μM)
BMB
hSK3
D
0
-8
-16
I (nA)
NS309
GW542573X (0.1 μM)
GW542573X (1 μM)
GW542573X (10 μM)
ChTX
2 min
hIK
E
20
10
0
Relative current
GW542573X (0.1 μM)
GW542573X (1 μM)
GW542573X (10 μM)
NS309 (0.1 μM)
hSK1
hSK2
hSK3
hIK

Figure 3

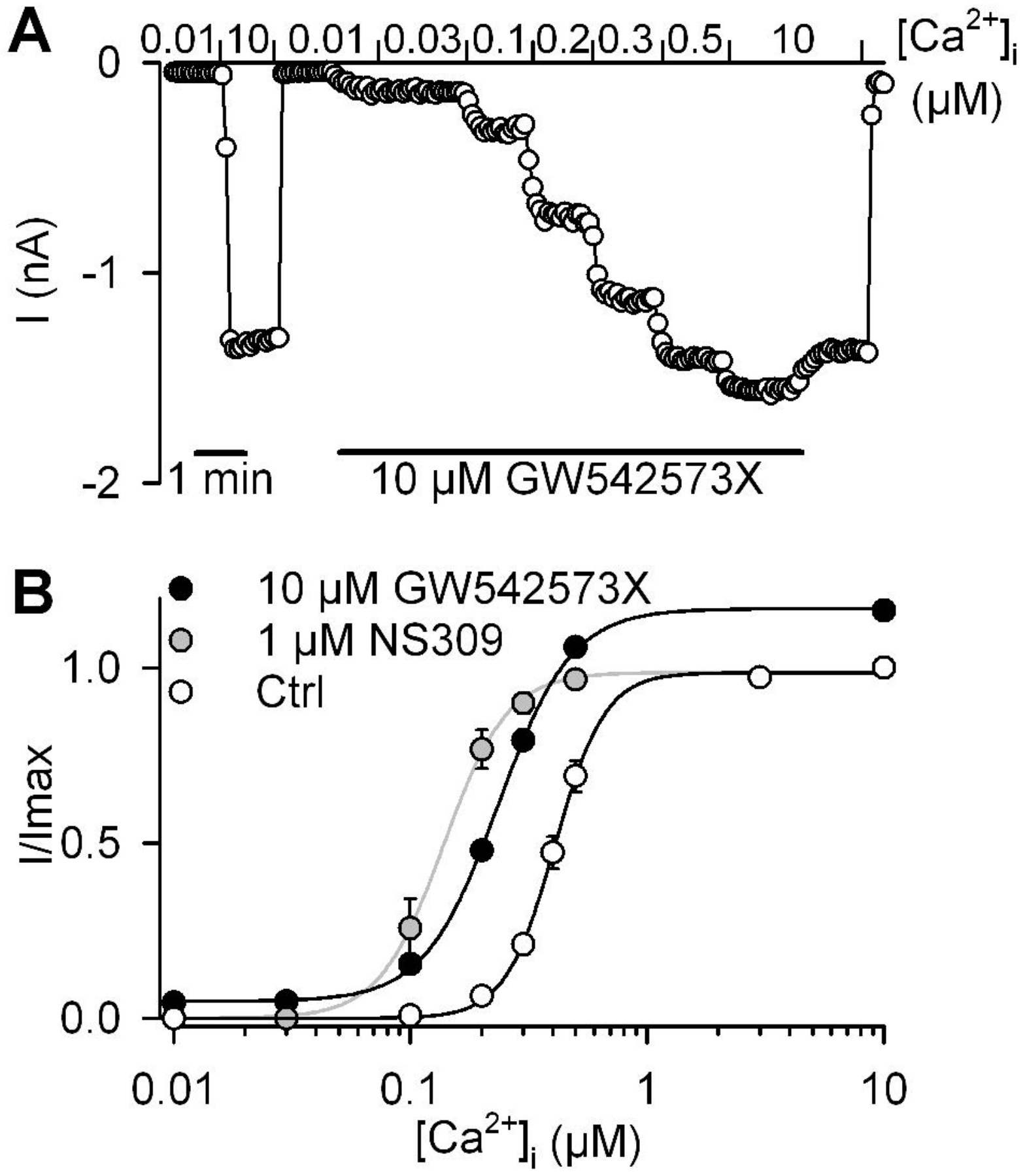
A
0.01
10
0.01
0.03
0.1
0.2
0.3
0.5
10
[Ca2+]i (μM)
0
-1
-2
I (nA)
1 min
10 μM GW542573X
B
10 μM GW542573X
1 μM NS309
Ctrl
1.0
0.5
0.0
I/Imax
0.01
0.1
1
10
[Ca2+]i (μM)

Figure 4

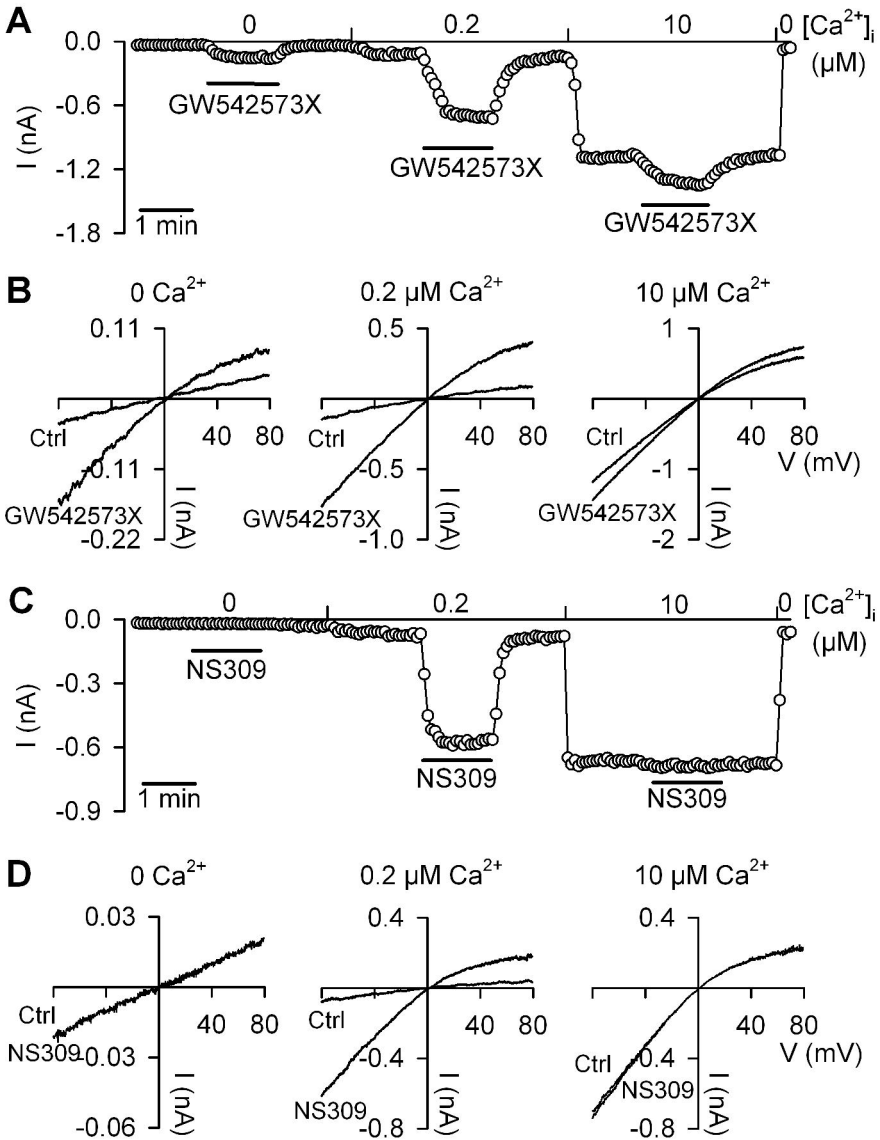
A
0
0.2
10
0 [Ca2+]i
(μM)
0.0
-0.6
-1.2
-1.8
I (nA)
GW542573X
GW542573X
GW542573X
1 min
B
0 Ca2+
0.2 μM Ca2+
10 μM Ca2+
0.11
0.5
1
Ctrl
40
80
-0.11
-0.5
-1
V (mV)
GW542573X
-0.22
-1.0
-2
I (nA)
C
0
0.2
10
0 [Ca2+]i
(μM)
0.0
-0.3
-0.6
-0.9
I (nA)
NS309
NS309
NS309
1 min
D
0 Ca2+
0.2 μM Ca2+
10 μM Ca2+
0.03
0.4
0.4
Ctrl
40
80
NS309
-0.03
-0.4
-0.4
V (mV)
-0.06
-0.8
-0.8
I (nA)

Figure 5

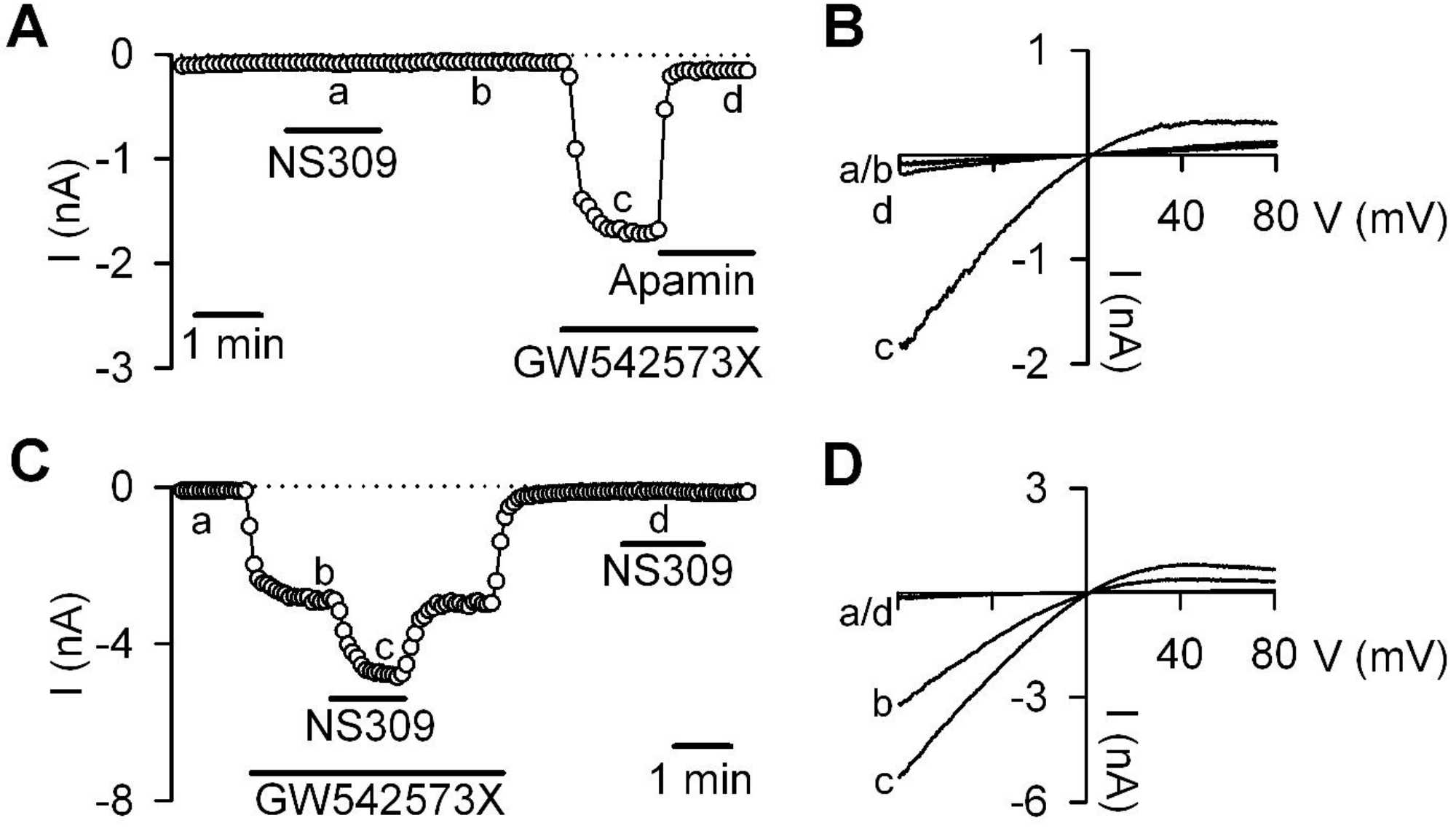
A
0
-1
-2
-3
I (nA)
a
b
c
d
NS309
Apamin
1 min
GW542573X
B
1
a/b
d
c
40
80 V (mV)
-1
-2
I (nA)
C
0
-4
-8
I (nA)
a
b
c
d
NS309
NS309
GW542573X
1 min
D
3
a/d
b
c
40
80 V (mV)
-3
-6
I (nA)

Figure 6

A

Channel	NS309 30 nM	GW542573X 200 nM	n	GW542573X current increase normalized to NS309
	Fold current increase			0.6 0.8 1.0 1.2
SK1	1.99 ± 0.15	1.67 ± 0.15	5	
SK3	1.70 ± 0.10	1.00	3	
Chimera 1	1.93 ± 0.13	1.09 ± 0.04	6	
Chimera 2	1.65 ± 0.08	1.47 ± 0.06	6	
Chimera 3	1.66 ± 0.06	1.69 ± 0.09	3	
Chimera 4	1.78 ± 0.31	1.69 ± 0.32	3	
Chimera 5	2.03 ± 0.07	1.71 ± 0.19	4	
Chimera 6	1.69 ± 0.20	1.34 ± 0.06	4	
Chimera 7	1.58 ± 0.12	1.28 ± 0.02	5	
Chimera 8	1.61 ± 0.10	1.43 ± 0.18	3	
Chimera 9	1.76 ± 0.08	1.09 ± 0.04	6	
Chimera 10	1.73 ± 0.05	1.50 ± 0.13	6	

B

```
hSK1  VFLISLELAVCAIHPVPGHYRFTWTARLAFTYAPSVAEADVDVLLSIPMFLRLYLLGRVMLLHSKIFTDASSRSIGALNKITFNTRFVMKTLMTICPGTVLLVFSISSWII
hSK3  ILYISLEMLVCAIHPIPGEYKFFWTARLAFSYTPSRAEADVDIILSIPMFLRLYLIARVMLLHSKLFTDASSRSIGALNKINFNTRFVMKTLMTICPGTVLLVFSISLWII
```

Chimera 5 Chimera 6 Chimera 7 Chimera 8 Chimera 9

Figure 7

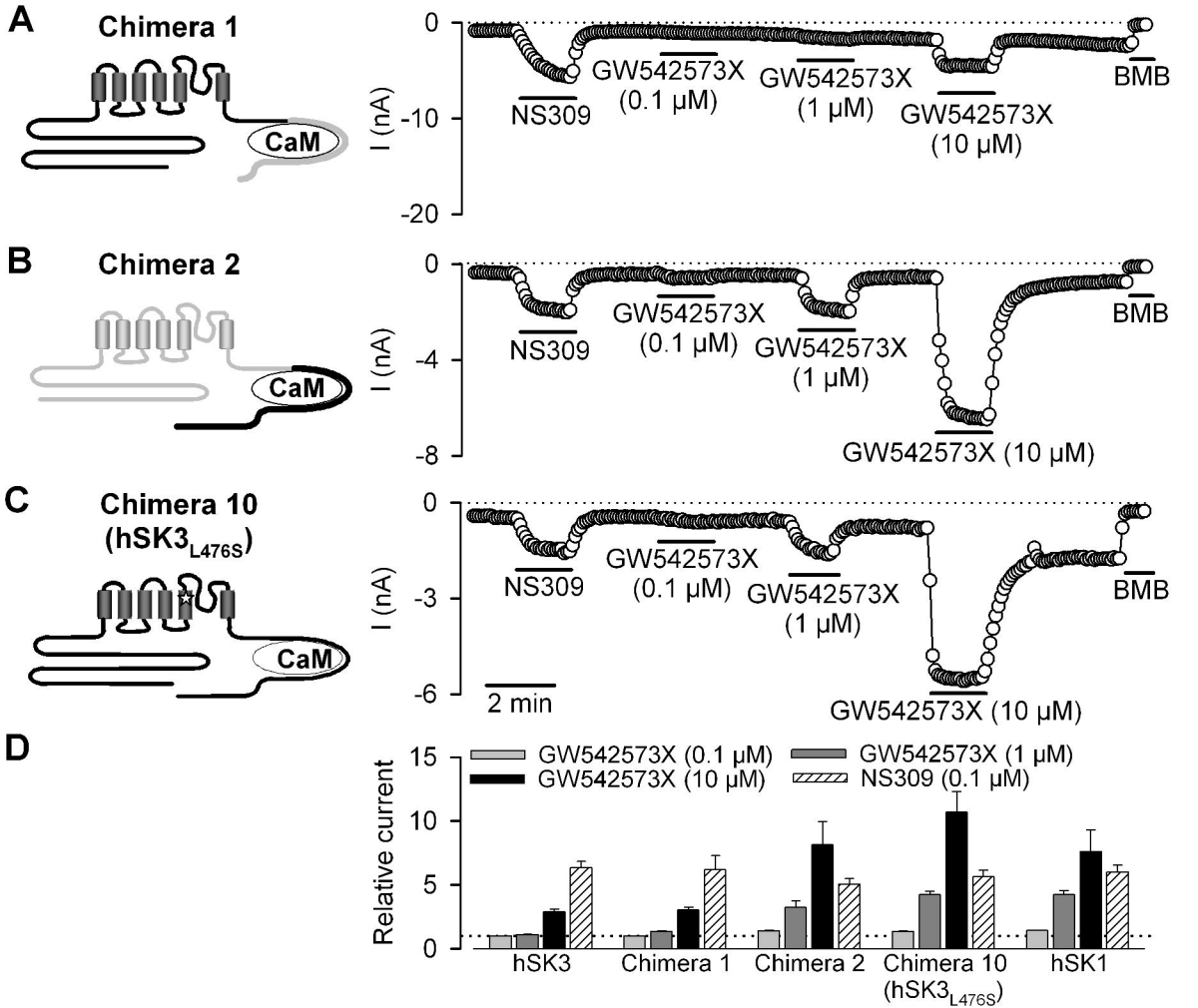
A
Chimera 1
CaM
0
-10
-20
I (nA)
NS309
GW542573X (0.1 μM)
GW542573X (1 μM)
GW542573X (10 μM)
BMB
B
Chimera 2
CaM
0
-4
-8
I (nA)
NS309
GW542573X (0.1 μM)
GW542573X (1 μM)
GW542573X (10 μM)
BMB
C
Chimera 10 (hSK3L476S)
CaM
0
-3
-6
I (nA)
NS309
GW542573X (0.1 μM)
GW542573X (1 μM)
GW542573X (10 μM)
BMB
2 min
D
GW542573X (0.1 μM)
GW542573X (1 μM)
GW542573X (10 μM)
NS309 (0.1 μM)
Relative current
15
10
5
0
hSK3
Chimera 1
Chimera 2
Chimera 10 (hSK3L476S)
hSK1

Figure 8

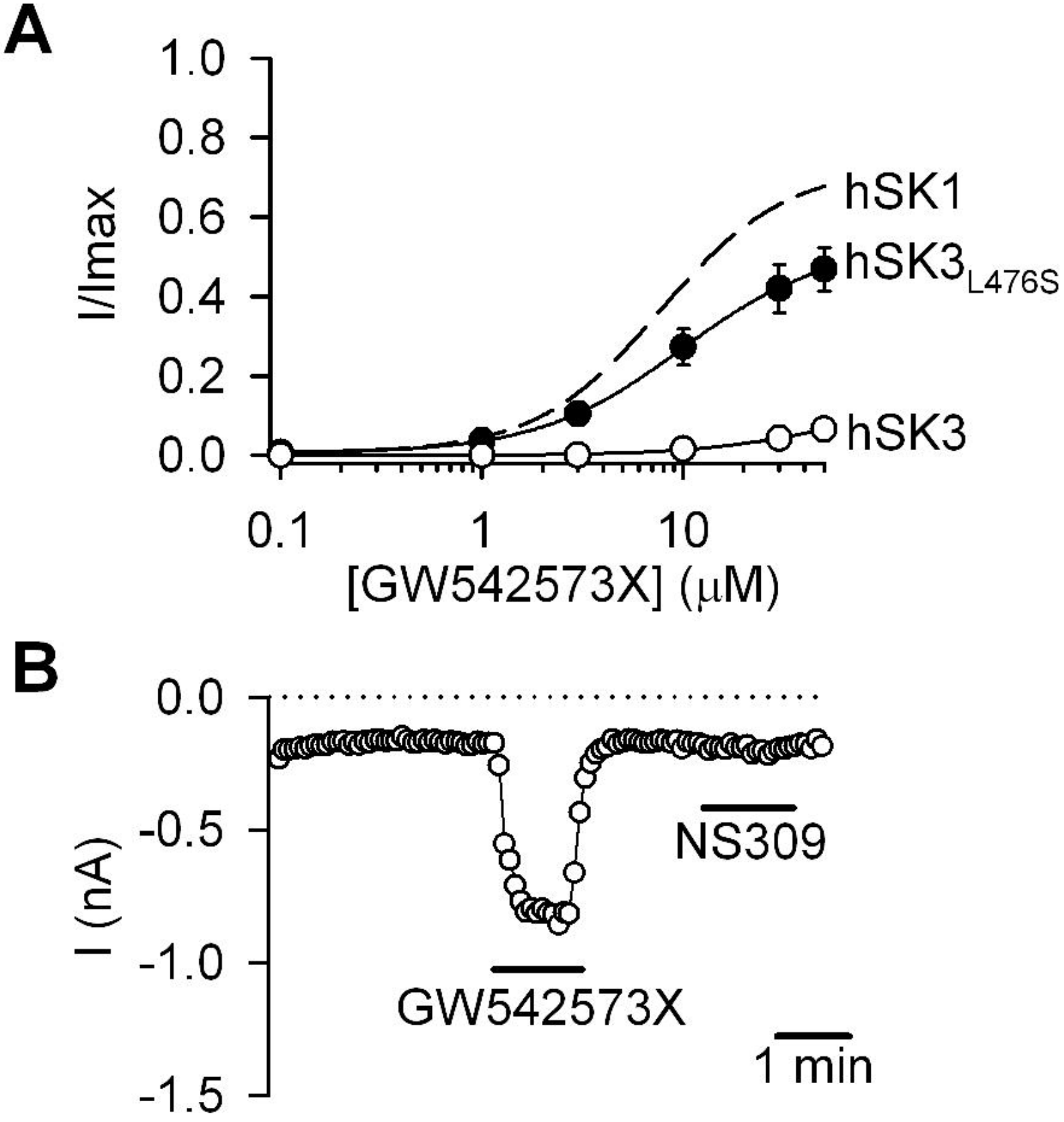
A
1.0
0.8
0.6
0.4
0.2
0.0
I/Imax
hSK1
hSK3L476S
hSK3
0.1
1
10
[GW542573X] (μM)
B
0.0
-0.5
-1.0
-1.5
I (nA)
NS309
GW542573X
1 min